DOI: 10.1002/ejic.200800615

The Supramolecular Architecture of Arene Complexes of Bis(polyfluorophenyl)-mercurials

Glen B. Deacon,*[a] Craig M. Forsyth,[a] Peter C. Junk,[a] Timothy J. Ness,[a] Ekaterina Izgorodina,[a] Jens Baldamus,[a] Gerd Meyer,[b] Ingo Pantenburg,[a,b] Julia Hitzbleck,[a,c] and Karin Ruhlandt-Senge[c]

Keywords: Supramolecular / Mercury / Arene / Fluorocarbon

The 1:1 (arene)mercury complexes [HgR_2(arene)] [R = C_6F_4-*o*-NO_2, C_6F_4-*m*-NO_2, C_6F_4-*o*-H, C_6F_5; arene = TMB (1,2,4,5-tetramethylbenzene), PMB (1,2,3,4,5-pentamethylbenzene)] are readily formed when mixtures of the mercurial and arene are crystallised from CH_2Cl_2 or CH_2Cl_2/hexane. Analogous 1:1 complexes are also formed from $Hg(C_6F_5)_2$ and PhMe, whereas novel 1:2 complexes [HgR_2(arene)$_2$] result from $Hg(C_6F_4$-*o*-$NO_2)_2$ and PhMe or TMO (1,2,4-trimethoxybenzene) and from $Hg(C_6F_5)_2$ and TMO. In the crystalline state, the 1:1 [HgR_2(arene)] complexes exist as canted columns of alternating planar HgR_2 and arene layers linked by weak (Hg···C 3.2–3.5 Å) η^1 or η^2 π-arene–mercury interactions. For the TMB (R = C_6F_4-*o*-NO_2, C_6F_4-*o*-H, C_6F_5) and PhMe (R = C_6F_5) complexes, the packing of neighbouring columns shows aligned, alternating fluoroarene and arene ring planes resulting in a 2D brick-wall motif with potential supramolecular components (fluoroarene–fluoroarene and fluoroarene–arene stacking). For the TMB complex with R = C_6F_4-*m*-NO_2 the 2D array is distorted into a herringbone motif by weak C–H···O interactions. The 1:2 complex [$Hg(C_6F_4$-*o*-$NO_2)_2$-$(PhMe)_2$] has an analogous mercury environment to the 1:1 complexes, and the packing shows a distinct layer structure of alternating rows of PhMe and HgR_2 with two PhMe units per HgR_2 unit but with no inter-stack interactions. The TMO complexes have long Hg···O contacts (3.2 Å) rather than Hg···C and similarly show a layered structure, but in this case, with a single column of alternating HgR_2 and pairs of TMO. Theoretical calculations for the 1:2 [$HgR_2(TMB)_2$] complexes (R = C_6F_4-*o*-NO_2, C_6F_4-*m*-NO_2) are consistent with the findings from the observed crystal structures.

Introduction

Perfluoroaryl groups, and in particular the pentafluorophenyl group, have long held a unique place in main group organometallic chemistry.[1a] The electron-withdrawing effect of fluorine substitution has been exploited to enhance Lewis acidity [with widespread application, e.g. $B(C_6F_5)_3$ "activators" for homogeneous olefin polymerisation catalysts[1b,1c]]. Pentafluorophenyl organometallic compounds also have been at the forefront of unusual main group and Cu organometallic donor–acceptor complexes, e.g. unsupported binding of arenes in [$Zn(C_6F_5)_2(\eta^2$-PhMe)], [$\{Cu(C_6F_5)\}_4(\eta^2$-$PhMe)_2$] and [$Al(C_6F_5)_3(\eta^1$-PhMe)].[2] The air-stable mercury complex $Hg(C_6F_5)_2$ is one of the simplest organometallic species to prepare and can be isolated in multi-gram quantities from commercial reagents in 1 h.[3] It is a sufficiently strong Lewis acid to sequester halide anions,[4a,4b] and recently Gabbaï and co-workers have demonstrated the formation of the arene complexes [$Hg(C_6F_5)_2$-(arene)] with naphthalene, biphenyl and fluorene.[4c] These mercury–arene complexes compliment the remarkable earlier work of Gabbaï with [$Hg(o$-$C_6F_4)]_3$ which forms "supramolecules" with numerous arenes,[5] as shown by the prototype [$\{Hg(o$-$C_6F_4)\}_3(C_6H_6)$] which contains a unique μ-η^2:η^2:η^2:η^2:η^2-C_6H_6 moiety.[5a]

A significant feature of (pentafluorophenyl)metal complexes has been the recognition of the potential for supramolecular chemistry by analogy with the intermolecular building blocks in organic chemistry.[6] Well-established elements of supramolecular chemistry such as offset face-to-face (*off*) or edge-to-face (*ef*) interactions of pairs of fluoroaromatic rings, parallel fluoroarene–arene assemblies, and N–H···F hydrogen bonds have been detected in the complexes $E(C_6F_5)_3$ or $E(C_6F_5)_4$ (E = group 13–15 elements),[7a] [$Zn(C_6F_5)_2$],[7b] arylamine adducts of (pentafluorophenyl)-zinc,[7c] boron,[7d] and aluminium.[7e] Analysis of the reported structures of bis(polyfluorophenyl)mercury compounds shows many instances of parallel fluoroarene–fluoroarene and fluoroarene–arene organization.[8,9] Consequently, in the (arene)mercury complexes [$Hg(C_6F_5)_2$-

[a] School of Chemistry, Monash University, Clayton, Victoria 3800, Australia
Fax: +613-99054597
E-mail: glen.deacon@sci.monash.edu.au
[b] Institut für Anorganische Chemie, Universität zu Köln, Köln, Germany
[c] Department of Chemistry, University of Syracuse, Syracuse, NY, USA
Supporting information for this article is available on the WWW under http://www.eurjic.org or from the author.

(arene)],[4c] fluoroarene–arene interactions are possible as a structural feature, similar to those in the solid binary phase formed on mixing equimolar amounts of liquid C_6H_6 and C_6F_6.[10] Much of the focus of the [$Hg(C_6F_5)_2$(arene)] and [{$Hg(o\text{-}C_6F_4)$}$_3$(arene)] molecules[4c,5] has been on the long mercury–carbon interactions (ca. 3.2–3.5 Å) which are just within the sum of the van der Waals radii of mercury (1.7–2.2 Å)[11a–11d] and an aromatic carbon atom (1.7 Å).[11e] Similar mercury–arene contacts (both intra- or intermolecular) have also been observed in organomercury compounds that have aryl substituents and are generally >3.2 Å.[12] However, these Hg···C distances are much longer than for molecular inorganic (arene)mercury complexes [$Hg_2(O_2CCF_3)_4(\eta^2\text{-}C_6Me_6)_2$] (2.56, 2.58 Å)[13a] or [$Hg(arene)_2(MCl_4)_2$] [M = Ga, Al; arene = C_6H_5Me, C_6H_5Et, 1,2-$C_6H_4Me_2$, 1,2,3-$C_6H_3Me_3$, (2.27–2.74 Å)].[13b,13c] The long Hg···C distances suggest only very weak interactions between the mercury centre and the arene rings, and consequently the supramolecular organization within the crystal may be a significant stabilization factor. The toluene solvate of ZnTPP (TPP = tetraphenylporphinate) has similarly long (3.121, 3.379 Å) M···C(PhMe) distances, and the parallel disposition of the arene and metal porphinate core suggested that the arene unit was held in place by both interaction with the metal atom and π-stacking with the porphinato ligand.[14] Notably, the [$Hg(C_6F_5)_2$(biphenyl)] complex does exhibit an additional fluoroarene–arene interaction with the second phenyl ring with a centroid–centroid distance of 3.65 Å.[4c]

We now report the preparation, crystal structures and theoretical calculations for arene complexes of $Hg(C_6F_4\text{-}o\text{-}NO_2)_2$ and $Hg(C_6F_4\text{-}m\text{-}NO_2)_2$ together with some comparable chemistry of $Hg(C_6F_5)_2$ and $Hg(C_6F_4\text{-}o\text{-}H)_2$ to explore further the various structural influences in these molecules. Introduction of the strongly electron-withdrawing nitro substituent should modify and enhance the Lewis acidity of the mercurial [encouraging arene(mercury) coordination] as well as introducing possible steric effects. The potential for mercury–nitro coordination (intra- or intermolecular) provides a further interesting feature.

Results and Discussion

Synthesis of (Arene)mercury (1:1) Complexes [HgR_2(arene)]

Addition of the moderately bulky methyl-substituted arenes 1,2,4,5-tetramethylbenzene (TMB) and 1,2,3,4,5-pentamethylbenzene (PMB) as solutions in CH_2Cl_2 or CH_2Cl_2/hexane to solutions of HgR_2 (R = $C_6F_4\text{-}o\text{-}NO_2$, $C_6F_4\text{-}m\text{-}NO_2$, C_6F_5, $C_6F_4\text{-}o\text{-}H$) in CH_2Cl_2 at room temperature followed by slow concentration gave pale yellow to colourless crystals of the corresponding 1:1 [HgR_2(arene)] complexes in good yields (Scheme 1). An analogous reaction of $Hg(C_6H_3\text{-}2,6\text{-}F_2)_2$ with TMB failed to yield a (arene)mercury complex. Similarly, reactions of $HgPh_2$ with the fluoroarenes $C_6F_4\text{-}p\text{-}H_2$ or $C_6F_5C_6F_5$ gave only the starting mercurial. The isolation of crystals of the 1:1 toluene complex [$Hg(C_6F_5)_2$(PhMe)] occurred upon crystallisation of the precursor from toluene, but the complex was unstable (giving [$Hg(C_6F_5)_2$] from rapid loss of PhMe). Apart from the PhMe complex, the other products gave satisfactory elemental analyses and were characterised by m.p., IR spectroscopy, X-ray crystallography, and, for selected examples, ^{13}C CPMAS NMR spectra and TGA data.

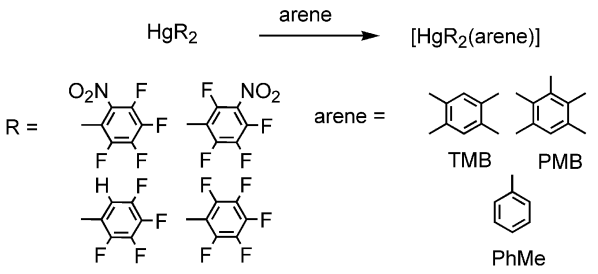

Scheme 1. Synthesis of 1:1 (arene)Hg complexes [HgR_2(arene)] from excess arene in CH_2Cl_2/hexane solutions (except for arene = PhMe, no additional solvent).

(Arene)mercury coordination was detected from the IR spectra of the products. For example, out of plane (*oop*) C–H deformation bands of TMB (866 cm^{-1}) or PMB (861 cm^{-1}) are shifted to higher energies in the corresponding (arene)mercury complexes, e.g. [$Hg(C_6F_4\text{-}o\text{-}NO_2)$-(TMB)] (878 cm^{-1}), [$Hg(C_6F_4\text{-}m\text{-}NO_2)$(TMB)] (890 cm^{-1}), [$Hg(C_6F_5)$(TMB)] (882 cm^{-1}), [$Hg(C_6F_4\text{-}o\text{-}H)$(TMB)] (880 cm^{-1}), and [$Hg(C_6F_4\text{-}m\text{-}NO_2)_2$(PMB)] (887 cm^{-1}). However, the changes in the TMB absorptions are smaller than that (46 cm^{-1}) observed for shifts in the C–H deformation frequency of benzene upon coordination to [$Hg(o\text{-}C_6F_4)]_3$.[5a] Some changes in the $C_6F_4\text{-}o\text{-}NO_2$ or $C_6F_4\text{-}m\text{-}NO_2$ absorptions are also observed with small shifts (ca. 10 cm^{-1} to higher energies) in the ν_{as}(N–O) frequencies (ca. 1540 cm^{-1} for the $o\text{-}NO_2$ complex and ca. 1550 cm^{-1} for the $m\text{-}NO_2$ complex) compared to those of the precursor mercurials.[15] TGA data for the TMB complex [$Hg(C_6F_4\text{-}m\text{-}NO_2)_2$(TMB)] showed a single-step mass loss of 18.0%, corresponding to elimination of TMB (calcd. 18.6%), occurring at 150–200 °C. This compares well with the trend for [{Hg-o-(C_6F_4)}$_3$(arene)] complexes where mass loss began at below 50 °C for the PhMe and 1,2- or 1,3-$Me_2C_6H_4$ derivatives, but at 91 °C for the 1,3,5-$Me_3C_6H_3$ complex.[5c] The solid-state ^{13}C CPMAS NMR resonances of the aromatic carbon atoms of TMB in [HgR_2 (TMB)] (R = $C_6F_4\text{-}m\text{-}NO_2$, C_6F_5) were only slightly deshielded (ca. 1–2 ppm) with respect to free TMB, consistent with observations for benzene in [{$Hg(o\text{-}C_6F_4)$}$_3(C_6H_6)$][4c] and indicative of weak mercury–arene coordination. By comparison, the much more strongly bound arenes in [$Hg(arene)_2(MCl_4)_2$] display significant shielding effects (ca. 30 ppm) for the mercury-bound carbon atoms[13b,13c] {see also NMR spectroscopic data for related [$Hg(arene)_2(SbF_6)_2$] compounds[13d–13f]}.

The crystal structure of [$Hg(C_6F_4\text{-}o\text{-}NO_2)_2$(TMB)] (Figure 1) exhibits a near planar HgR_2 unit, and one oxygen atom of each of the nitro groups forms a short intramolecular Hg–O interaction in a *transoid* orientation. The Hg–O bond (Figure 2) is marginally shorter than for an

analogous interaction in $[Hg(C_6H_4\text{-}o\text{-}P(O)Ph_2)_2]$ [Hg–O 2.874(5) Å].[16] In contrast, shorter Hg–O bonds are observed in $[Hg(C_6F_5)Cl(L)]$ [L = dmso: 2.542(4) Å],[17] consistent with the stronger acceptor properties for HgArCl derivatives than for the corresponding $HgAr_2$ compounds. The Hg–C(C_6F_4-*o*-NO_2) distance is comparable to those of known bis(polyfluorophenyl)mercurials[9] and is not lengthened significantly by arene coordination. Overall, the metrical parameters of the $Hg(C_6F_4\text{-}o\text{-}NO_2)_2$ unit in the TMB complex are similar to those of the isolated precursor.[15c] In $[Hg(C_6F_4\text{-}o\text{-}NO_2)_2(TMB)]$ the TMB moiety is located above the mercury atom and approximately parallel to the HgR_2 plane (interplanar angle 3.4°). As required by crystal symmetry, in each molecular unit of $[Hg(C_6F_4\text{-}o\text{-}NO_2)_2(TMB)]$ the mercury atom forms part of an infinite, step-like chain of alternating HgR_2 and TMB molecules (with equidistant Hg···C(TMB) interactions, see below).

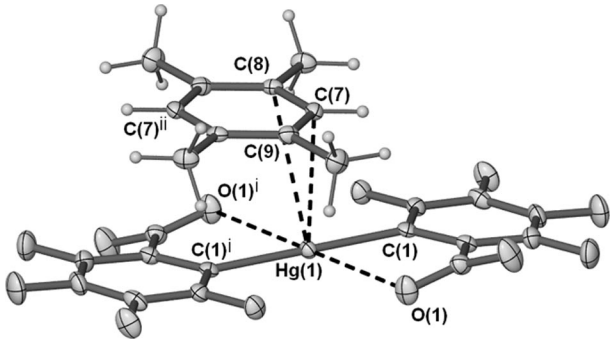

Figure 1. Molecular diagram of $[Hg(C_6F_4\text{-}o\text{-}NO_2)_2(TMB)]$ shown with 50% thermal ellipsoids and hydrogen atoms as spheres of arbitrary size. Selected bond lengths [Å] and angles [°]: Hg(1)–C(1) 2.084(2), Hg(1)–O(1) 2.769(2), Hg(1)–C(7) 3.152(3), Hg(1)–C(8) 3.298(3); C(1)–Hg(1)–C(1^i) 180.0, O(1)–Hg(1)–O(1^i) 180.0, C(7)–Hg(1)–C(7^i) 180.0. Symmetry operators: i: –*x*, –*y*, –*z*; ii: –*x*, 1 – *y*, –*z*.

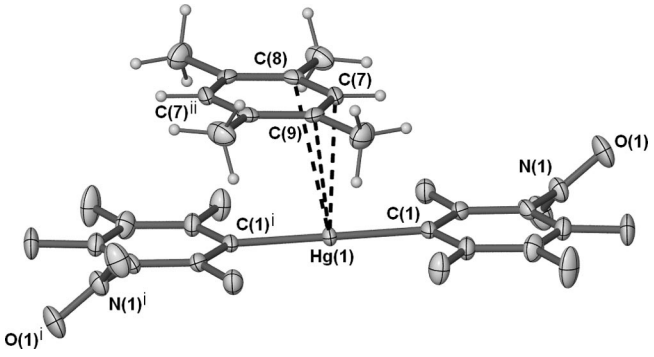

Figure 2. Molecular diagram of $[Hg(C_6F_4\text{-}m\text{-}NO_2)_2(TMB)]$ shown with 50% thermal ellipsoids and hydrogen atoms as spheres of arbitrary size. Selected bond lengths [Å] and angles [°]: Hg(1)–C(1) 2.071(3), Hg–C(7) 3.097(3), Hg(1)–C(8) 3.385(3), Hg(1)–C(9) 3.426(3); C(1)–Hg(1)–C(1^i) 180.0, C(7)–Hg(1)–C(7^i) 180.0. Symmetry operators: i: –*x*, –*y*, –*z*; ii: –*x*, 1 – *y*, –*z*.

In the structure of $[Hg(C_6F_4\text{-}m\text{-}NO_2)_2(TMB)]$ (Figure 2) the planar $Hg(C_6F_4\text{-}m\text{-}NO_2)_2$ molecule has the *m*-NO_2 groups in a *transoid* orientation and the TMB moiety located above the mercury atom (interplanar angle 2.8°). There are no intramolecular Hg–O interactions with the *m*-NO_2 groups which are twisted out of the C_6 plane {torsion angle 133.5(4)°, cf. 157.4(3)° for $[Hg(C_6F_4\text{-}o\text{-}NO_2)_2(TMB)]$}. The Hg–C($C_6F_4$-*m*-$NO_2$) distances are virtually identical with those of the *o*-NO_2 complex above. However, the planar $Hg(C_6F_4\text{-}m\text{-}NO_2)_2$ unit contrasts that of the uncomplexed mercurial, which has a twisted (interplanar angle 87.3°) configuration.[15c]

For the structures of both TMB complexes, the closest Hg···C distances are within, or below, the range observed in $[\{Hg(o\text{-}C_6F_4)\}_3(C_6H_6)]$, 3.25–3.55 Å.[4c] For the *o*-NO_2 complex, these distances define an η^2 interaction (Figure 1), but the Hg···C distances are not symmetrical with that to the C(Me) being ca. 0.15 Å longer, possibly due to the steric bulk of the attached Me group (see below). In contrast, the TMB molecule in the *m*-NO_2 complex (Figure 2) shows one close contact to the C(H) carbon atom and two more distant contacts to the neighbouring C(Me) carbon atoms ($\Delta \approx 0.3$ Å) suggesting an η^1 (or η^3) attachment (the longer distances are still within the bonding range of $\{[Hg(o\text{-}C_6F_4)]_3(C_6H_6)\}$; see above). The next nearest Hg···C distances are >> 3.5 Å for both complexes. The orientation of the arene ring in the $[Hg(C_6F_4\text{-}o\text{-}NO_2)_2(TMB)]$ complex, as defined by the torsion angle between the HC–CH axis of the TMB and the Hg–C(R) bond (15.4°), is such that the η^2-C–C···Hg interaction is approximately perpendicular to the C–Hg–C bonds, whereas for $[Hg(C_6F_4\text{-}m\text{-}NO_2)_2(TMB)]$ the corresponding angle is 5.7°, consistent with an η^1, rather than an η^2, attachment of the TMB molecule.

The other TMB complexes prepared in this study, $[Hg(C_6F_4\text{-}o\text{-}H)_2(TMB)]$ and $[Hg(C_6F_5)_2(TMB)]$, show closely related structures (see Supporting Information for full structural details) to those of the $[Hg(C_6F_4\text{-}o\text{-}NO_2)_2(TMB)]$ complex above. The geometry of the $Hg(C_6F_4\text{-}o\text{-}H)_2$ unit in the TMB complex is almost identical with that of the uncomplexed mercurial,[9b] whereas the similarly planar $Hg(C_6F_5)_2$ molecule in the corresponding TMB complex contrasts the twist angle of ca. 60° between the fluoroaryl rings of uncomplexed $Hg(C_6F_5)_2$.[9c,9d] The Hg···C(TMB) distances for $[Hg(C_6F_4\text{-}o\text{-}H)_2(TMB)]$ and $[Hg(C_6F_5)_2(TMB)]$, are listed in Table 1 and indicate an η^2 attachment of the TMB to the mercury atom, similar to the orientation observed for the *o*-NO_2 derivative (above). The PMB complex $[Hg(C_6F_4\text{-}m\text{-}NO_2)_2(PMB)]$ (see Supporting Information for full structural details) forms an analogous structure to that of the *m*-NO_2 TMB complex above (with the PMB 50:50 disordered with respect to the position of the CH), but with marginally longer Hg···C distances (Table 1). The structure of the 1:1 PhMe complex, $[Hg(C_6F_5)_2(PhMe)]$ (Figure 3), is closely related to those of the other 1:1 complexes above. In the current structure, the toluene molecule is disordered and the two components related by an inversion centre. The Hg···C distances are of the same order of magnitude to those above and define an η^2 interaction to the mercury atom (Figure 3) [the second component of the disordered PhMe unit has only one shorter Hg···C distance of 3.18(2) Å to C(11)].

Table 1. Selected Hg···C distances (< 3.6 Å) in (1:1) [HgR_2(arene)] complexes. The atom labelling scheme for the C atoms follows that of [Hg(C_6F_4-*o*-NO_2)(TMB)] above.

	R	Arene	Hg(1)–C(7)	Hg(1)–C(8)	Hg(1)–C(9)
a	C_6F_4-*o*-NO_2	TMB	3.152(3)	3.298(3)	
b	C_6F_4-*m*-NO_2	TMB	3.097(3)	3.385(3)	3.426(3)
c	C_6F_5	TMB	3.154(5)	3.268(5)	
d	C_6F_4-*o*-H	TMB	3.188(5)	3.280(4)	
e	C_6F_4-*m*-NO_2	PMB	3.266(4)	3.544(4)	3.550(4)
f	C_6F_5	PhMe	3.26(2)[a]	3.319(9)	

[a] In the second component of the PhMe disorder, there is an η^1-C···Hg interaction to C(11) with a distance of 3.18(2) Å.

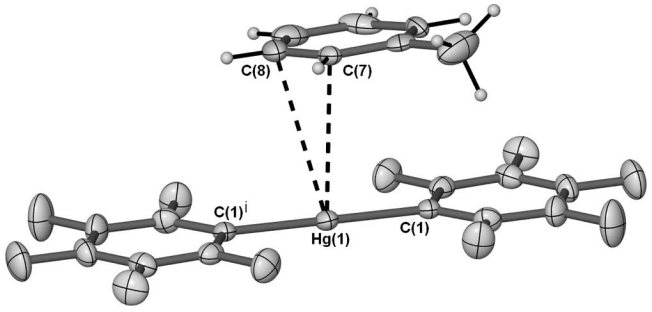

Figure 3. Molecular diagram of [Hg(C_6F_5)$_2$(PhMe)], shown with 50% thermal ellipsoids and hydrogen atoms as spheres of arbitrary size. Only one component of the disordered PhMe molecule is shown. Selected bond lengths [Å] and angles [°]: Hg(1)–C(1) 2.069(3), Hg(1)···C(7) 3.26(2), Hg(1)···C(8) 3.319(9); C(1)–Hg(1)–C(1^i) 180.0. Symmetry operators: ^{i}: –*x*, –*y*, –*z*.

In the [HgR_2(arene)] complexes above, individual molecules are assembled into infinite stacks by repetition of the Hg–arene interactions as required by crystallographic symmetry [inversion centres located at Hg(1) and the centroid of the arene in each structure] and translation along the *a* (structures **c** and **d**, Table 1) or *b* (structures **a**, **b** and **f**, Table 1) axis directions (e.g. [Hg(C_6F_5)$_2$(TMB)] Figure 4). Each mercury atom is coordinated to two TMB molecules, one above and one below the HgR_2 plane, and each TMB molecule is bound to two mercury atoms. These interactions result in an infinite, step-like chain of alternating HgR_2 and TMB molecules. Due to crystallographic symmetry, the Hg···C distances are identical to those for the individual complexes and define equivalent coordination modes [except for the case of the PhMe complex (structure **f**) which, for each of the two disordered PhMe positions, has two contacts to one Hg atom, and one shorter Hg···C contact to the neighbouring Hg atom].

The columns of [HgR_2(TMB)]$_n$ also pack into 2D sheets. For all but the *m*-NO_2 complex, the protruding fluoroarene rings of each individual stack interleave with the neighbouring stacks on either side, offset by one layer (Figure 5). The overall packing manifests as a brick wall motif which shows significant alignment of pairs of fluoroarene rings from neighbouring stacks. The interplanar separation is approximately 3.35 Å in all the structures, but the degree of overlap of the fluoroarene rings for the *o*-NO_2-TMB complex is reduced as compared with the C_6F_5-TMB and C_6F_5-PhMe

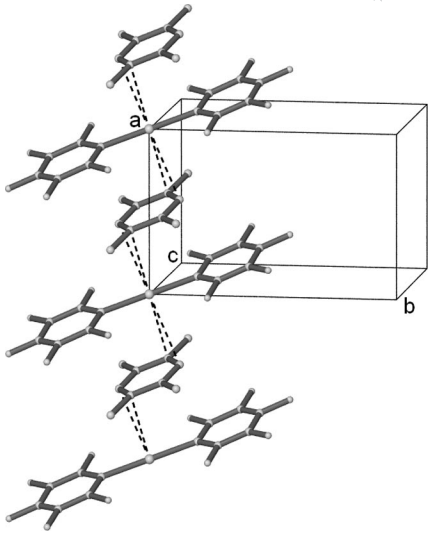

Figure 4. Ball-and-stick representation of [Hg(C_6F_5)$_2$(TMB)] showing the assembly of molecular HgR_2(arene) units into a stepped vertical stack.

complexes (Figure 6). Within each layer of the [HgR_2(TMB)] (R = C_6F_4-*o*-NO_2, C_6F_5) packing, successive coplanar TMB and fluoroarene rings are separated by C–H···F distances of ca. 2.51 Å (to the TMB CH_3 in the C_6F_4-*o*-NO_2 complex or to the TMB CH in the C_6F_5 complex) which may constitute structural contacts (C–H···F ca. 150°). The significance of C–H···F–C interactions in crystal engineering is debateable due to the poor acceptor properties of organofluorine moieties, and it has been proposed that, at a minimum, such "interactions" should be limited to those within the sum of the van der Waals radii (2.55 Å).[18] Contact distances of ca. 2.40 Å have been associated with spectroscopically observable NMR coupling in

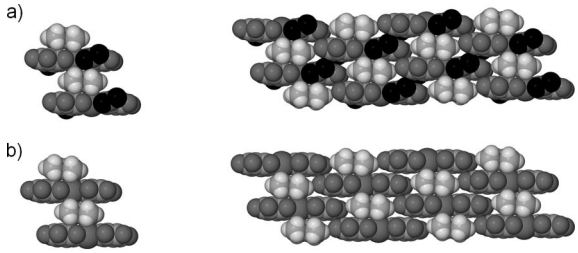

Figure 5. Individual stacks of [HgR_2(arene)] and two-dimensional packing of neighbouring chains showing a brick wall motif. (a) [Hg(C_6F_4-*o*-NO_2)$_2$(TMB)] and (b) [Hg(C_6F_5)$_2$(TMB)] {[Hg(C_6F_4-*o*-H)$_2$(TMB)] and [Hg(C_6F_5)$_2$(PhMe)] show analogous packing}. Atoms are represented as van der Waals spheres (HgR_2 dark; arene light).

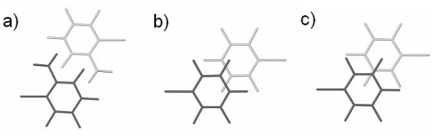

Figure 6. The major *off* fluoroarene–fluoroarene stacking in (a) [Hg(C_6F_4-*o*-NO_2)$_2$(TMB)], (b) [Hg(C_6F_5)$_2$(TMB)] and (c) [Hg(C_6F_5)$_2$(PhMe)] as viewed perpendicular to the C_6F_5 plane.

solution and in the solid state,[19] but we were unable to obtain satisfactory ^{19}F MAS NMR spectra. Intriguingly, in the packing of the *m*-NO_2 derivative, [Hg(C_6F_4-*m*-NO_2)$_2$-(TMB)], there are analogous C–H···O contacts (ca. 2.52 Å) between the nitro groups and the TMB C–H bonds. As a result of the out-of-plane twisting of the nitro groups, this complex exhibits a significantly different two-dimensional packing with a herringbone motif (Figure 7) rather than planar layers as observed for the *o*-NO_2 and C_6F_5 structures. This packing also lacks the inter-stack *off* fluoroarene–fluoroarene arrangement of the other TMB complexes.

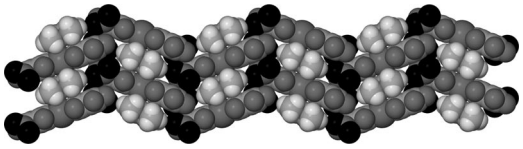

Figure 7. Two-dimensional packing of [Hg(C_6F_4-*m*-NO_2)$_2$(TMB)] showing a herringbone alignment of neighbouring chains. Atoms are represented by van der Waals spheres (HgR_2 dark; arene light).

Synthesis of (Arene)mercury (2:1) Complexes [HgR_2(arene)$_2$]

Contrary to the isolation of 1:1 (arene)mercury complexes above, and 1:1 arene complexes with [{Hg(*o*-C_6F_4)}$_3$],[4c,5] crystallisation of [Hg(C_6F_4-*o*-NO_2)$_2$] from toluene resulted in the isolation of the 1:2 complex, [Hg(C_6F_4-*o*-NO_2)$_2$(PhMe)$_2$]. The product was unstable with respect to loss of toluene preventing characterisation other than by X-ray crystallography. The composition was particularly surprising, given the formation of [Hg(C_6F_5)$_2$(PhMe)] (above) under similar conditions. During the preparation of [Hg(C_6F_4-*o*-NO_2)$_2$(TMB)], no evidence of a 1:2 stoichiometry was detected, despite the use of excess TMB in the reaction mixtures. However, stable 1:2 complexes [HgR_2-(arene)$_2$] [R = C_6F_4-*o*-NO_2 and C_6F_5; arene = 1,2,4-trimethoxybenzene (TMO)] were prepared from the respective mercurials and an excess of the arene in CH_2Cl_2/hexane (Scheme 2). The TMO complexes have been fully characterised and gave satisfactory elemental analyses. Significantly, the TMO complexes have lower melting points than the corresponding 1:1 TMB complexes. Only minor changes in the IR absorptions are observed for the TMO component with the ν(C–O) frequency shifted ca. 10 cm^{-1} to lower energies, whereas the *oop* γ(C–H) frequency is shifted ca. 5 cm^{-1} to higher energies. The ^{13}C CPMAS NMR spectrum of [Hg(C_6F_5)$_2$(TMO)$_2$] showed five resonances for the six aromatic carbon atoms and a single OMe resonance, each within 1–2 ppm of the chemical shift observed in the solution-state ($CDCl_3$) spectrum of pure TMO.

The structure of [Hg(C_6F_4-*o*-NO_2)$_2$(PhMe)$_2$] (Figure 8) shows similarities with the basic core of the 1:1 complexes. The HgR_2 unit is essentially the same as for the *o*-NO_2 TMB complex, with comparable intramolecular Hg–O bonds and slight twisting of the NO_2 group out of the C_6 plane {dihedral angle 28.4(7)°, cf. 23.4(2)° for [Hg(C_6F_4-*o*-NO_2)$_2$(TMB)]}. The Hg atom in [Hg(C_6F_4-*o*-NO_2)$_2$-(PhMe)$_2$] is coordinated to two PhMe molecules by η^2 interactions with the *para* carbon atoms and a *meta* carbon atom with Hg···C distances similar to those of the TMB complex above. However, the difference between the two unique Hg–C distances is somewhat larger (ca. 0.19 Å) than for the TMB complex, even though both carbon atoms are unsubstituted (cf. the TMB complex). Despite the differing stoichiometry of this complex, compared with the 1:1 (arene)mercury complexes, the structural data show a virtually identical mercury environment due to the vertical stacking of the individual [HgR_2(arene)] molecules in the 1:1 systems.

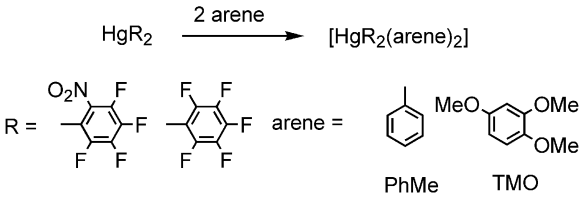

Scheme 2. Synthesis of 2:1 (arene)mercury complexes [HgR_2-(arene)$_2$] from excess arene in CH_2Cl_2/hexane (2:1) (except for arene = PhMe: no solvent).

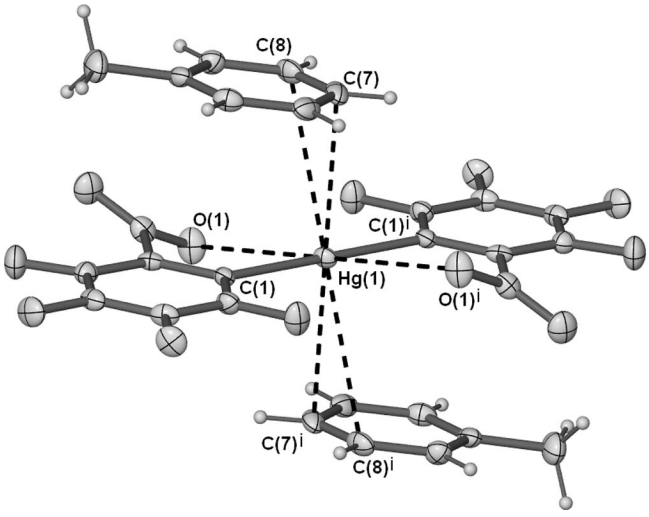

Figure 8. Molecular diagram of [Hg(C_6F_4-*o*-NO_2)$_2$(PhMe)$_2$] shown with 50% thermal ellipsoids. Selected bond lengths [Å] and angles [°]: Hg(1)–C(1) 2.076(7), Hg(1)–O(1) 2.873(6), Hg(1)–C(7) 3.136(8), Hg(1)–C(8) 3.327(8); C(1)–Hg(1)–C(1^i) 180.0, O(1)–Hg(1)–O(1^i) 180.0. Symmetry operators: ^{i}: 1 – *x*, 1 – *y*, 1 – *z*.

The TMO complexes [HgR_2(TMO)$_2$] (R = C_6F_4-*o*-NO_2, C_6F_5) have similar overall configurations. The *o*-NO_2 complex [Hg(C_6F_4-*o*-NO_2)$_2$(TMO)$_2$] (Figure 9) shows an HgR_2 unit, virtually identical to that observed in the TMB complex above, with intramolecular Hg–O coordination, and comparable Hg–C and Hg–O distances to those of the other Hg(C_6F_4-*o*-NO_2)$_2$ complexes. The two TMO molecules are located almost directly above and below the fluoroarene rings and are approximately parallel (dihedral angle 5.1°). The closest Hg···O(TMO) separation of 3.203(3) Å is

within the sum of the van der Waals radii of oxygen (1.54 Å)[11f] and mercury (1.73–2.2 Å).[11a–11d] Comparable Hg···O distances are observed in the oxygen donor complexes [{Hg(*o*-C_6F_4)}$_3$(L)] (ca. 2.85–3.25 Å)[20] and [Hg(C_6F_4-*p*-OH)$_2$(H_2O)] [3.127(8) Å],[9g] whereas longer intermolecular Hg···O contacts are reported in [Hg(C_6F_4-*p*-OMe)$_2$] (3.313 Å).[9e] The structure of [Hg(C_6F_5)$_2$(TMO)$_2$] is isotypic (see Supporting Information), with an HgR_2 moiety sandwiched between two TMO molecules. The shorter Hg···O(TMO) distance of 3.103(2) Å plausibly reflects both the lower steric bulk and lower mercury coordination number (4) in the absence of the *o*-NO_2 substituent. A notable feature of the two TMO complexes is the small step in the HgR_2 molecule. Thus, the two (inversion-related) fluoroarene rings are parallel, but not co-planar, with an interplanar separation of 0.38 Å (C_6F_4-*o*-NO_2 complex) or 0.56 Å (C_6F_5 complex). In comparison, the two C_6F_4 rings in [Hg(C_6F_4-*o*-NO_2)$_2$(PhMe)$_2$] are coplanar to within 0.01 Å.

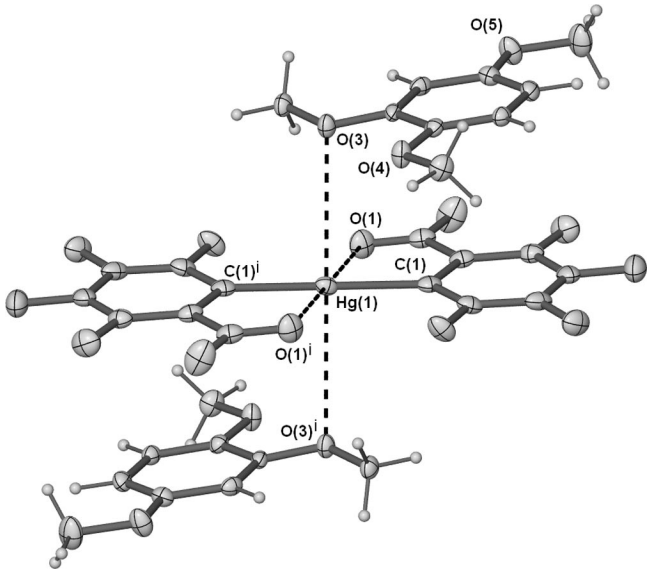

Figure 9. Molecular diagram of [Hg(C_6F_4-*o*-NO_2)$_2$(TMO)$_2$] shown with 50% thermal ellipsoids. Selected bond lengths [Å] and angles [°]: Hg(1)–C(1) 2.086(4), Hg(1)–O(1) 2.790(3), Hg(1)–O(3) 3.203(3); C(1)–Hg(1)–C(1^i) 180.0, O(1)–Hg(1)–O(1^i) 180.0. Symmetry operators: ^{i}: 1 – *x*, 1 – *y*, –*z*.

The packing of the 2:1 (arene)mercury complexes consists of infinite stacks comprising successive layers of HgR_2 and two *coplanar* PhMe or TMO molecules (Figure 10). In [Hg(C_6F_4-*o*-NO_2)$_2$(PhMe)$_2$], these stacks are arranged in a linear fashion (analogous to the brick wall motif of the 1:1 TMB complex; see above), but there is no interstack fluoroarene–fluoroarene overlap. The spatial arrangement of the stacks in the TMO complexes is more random reflecting the lack of interstack interactions in the 1:2 systems. However, within each stack there is significant overlap of the fluoroarene and arene (TMO) rings (Figure 11). The interplanar separation is approximately 3.3 Å for both complexes, and these represent supramolecular fluoroarene-arene interactions. In the TMO complexes, the pairs of TMO molecules are arranged such that the *ortho*-OMe groups are facing each other. In this position there are complementary weak C–H···O contacts (2.42 Å, C_6F_4-*o*-NO_2; 2.51 Å, C_6F_5) between one of the ether oxygen atoms and the methyl group of the methoxy substituent from the opposing TMO molecule.

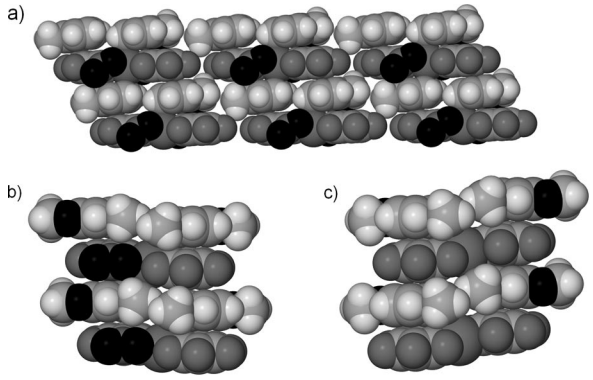

Figure 10. Two-dimensional packing of (a) [Hg(C_6F_4-*o*-NO_2)$_2$(PhMe)$_2$], (b) [Hg(C_6F_4-*o*-NO_2)$_2$(TMO)$_2$] and (c) [Hg(C_6F_5)$_2$(TMO)$_2$], showing the layered planar alignment of arenes and mercurials. Atoms are represented as van der Waals spheres (HgR_2 dark, arene light).

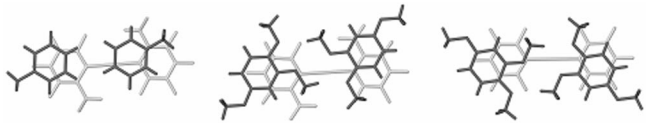

Figure 11. Degree of overlap of the fluoroarene and arene (PhMe or TMO) ring planes within successive HgR_2(arene)$_2$ layers, as viewed perpendicular to the fluoroarene plane. (a) [Hg(C_6F_4-*o*-NO_2)$_2$(PhMe)$_2$]; (b) [Hg(C_6F_4-*o*-NO_2)$_2$(TMO)$_2$]; (c) [Hg(C_6F_5)$_2$(TMO)$_2$].

Calculated Structures of [Hg(C_6F_4-*o*-NO_2)$_2$(TMB)$_2$] and [Hg(C_6F_4-*m*-NO_2)$_2$(TMB)$_2$]

We optimized the structures of the 1:2 [Hg(C_6F_4-*o*-NO_2)$_2$(TMB)$_2$] and [Hg(C_6F_4-*m*-NO_2)$_2$(TMB)$_2$] complexes as representative of the mercury environment in both the 1:1 and 1:2 systems. Having two TMB molecules present in the complex allowed us to use C_i symmetry and thus, a planar configuration of the aryl rings was kept during the optimization. In the case of the 1:2 [Hg(C_6F_4-*o*-NO_2)$_2$(TMB)$_2$] complex two configurations separated by only 1 kJ mol^{-1} were found (Figure 12). These configurations possess different types of mercury–TMB interactions, with the η^1-C–Hg arrangement being energetically marginally preferable to the η^2-C–C–Hg arrangement. In contrast, for the 1:2 [Hg(C_6F_4-*m*-NO_2)$_2$(TMB)$_2$] complex, only one configuration with the η^1-type interaction was found (Figure 13). The carbon atom on the TMB molecule has a shorter (ca. 0.1 Å) contact with the mercury atom compared with that in the 1:2 [Hg(C_6F_4-*o*-NO_2)$_2$(TMB)$_2$] complex. Attempts to rotate the TMB ring to achieve an η^2 arrangement only resulted

in the η^1 mercury–TMB coordination shown in Figure 13. The theoretical findings are in good qualitative agreement with the crystal structures for both $[Hg(C_6F_4\text{-}o\text{-}NO_2)_2(TMB)]$ and $[Hg(C_6F_4\text{-}m\text{-}NO_2)_2(TMB)]$. In both the calculated $[Hg(C_6F_4\text{-}o\text{-}NO_2)_2(TMB)_2]$ structures, the nitro groups are coordinated to the mercury atom with the Hg–O (2.774, 2.778 Å) distances close to those observed (see above). There is no analogous Hg–O bonding in the calculated $[Hg(C_6F_4\text{-}m\text{-}NO_2)_2(TMB)_2]$ structure, and the difference in the respective torsion angles for the out-of-plane twisting of the nitro groups between the $o\text{-}NO_2$ and $m\text{-}NO_2$ derivatives (158/160, 129°) is consistent with the crystal structure results (see above). However, the calculated Hg–C (2.155, 2.154, 2.132 Å) distances (for both complexes) are marginally longer than the observed values.

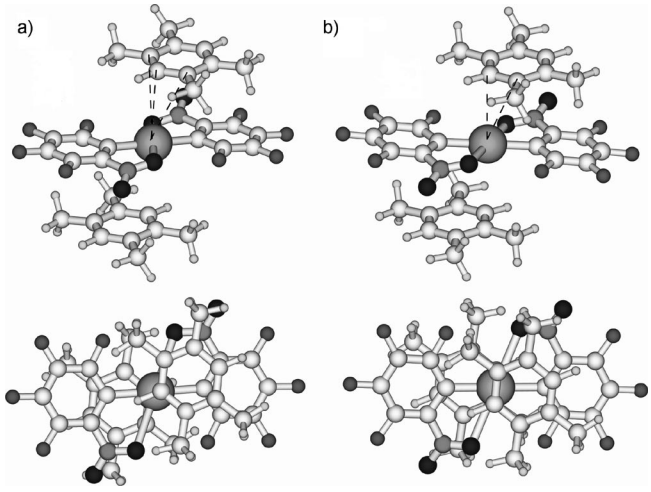

Figure 12. Optimized structures of the 1:2 $[Hg(C_6F_4\text{-}o\text{-}NO_2)_2(TMB)_2]$ complexes: (a) with an η^1/η^3 interaction between TMB and the Hg atom, calculated Hg–C 3.825, 3.537, 3.913 Å; (b) with an η^2 interaction between TMB and the Hg atom, calculated Hg–C 3.524, 3.767 Å. The bottom structures are shown as a view from above.

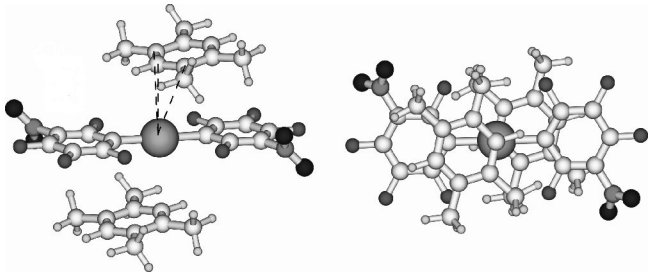

Figure 13. Optimized structure of the 1:2 $[Hg(C_6F_4\text{-}m\text{-}NO_2)_2(TMB)_2]$ complexes with an η^1/η^3 attachment between TMB and the Hg atom; calcd. Hg–C 3.716, 3.467, 3.880 Å.

The calculated η^1-TMB binding to the mercury atom in $[Hg(C_6F_4\text{-}m\text{-}NO_2)_2(TMB)_2]$ agrees well with the observed η^1 or η^3 coordination in $[Hg(C_6F_4\text{-}m\text{-}NO_2)_2(TMB)]$, in which there is a shorter (ca. 0.3 Å) contact to the middle carbon atom. This distance is also shorter (ca. 0.05–0.10 Å) than the η^2-TMB interaction observed in $[Hg(C_6F_4\text{-}o\text{-}NO_2)_2(TMB)]$, as predicted in the calculated $[Hg(C_6F_4\text{-}o\text{-}NO_2)_2(\eta^2\text{-}TMB)_2]$ structure. However, the Hg···C(TMB) distances derived from the theoretical structures are ca. 0.4 Å longer than the experimental values and are at, or beyond, the lower limit of the sum of the van der Waals radii (3.4–3.9 Å).[11a–11d] In comparison, the calculated structure of $[Hg(AlCl_4)_2(PhMe)_2]$ has an Hg–C distance significantly shorter (e.g. 2.382 Å), and only marginally longer (ca. 0.06 Å) than the experimentally observed values.[13b] Similarly, calculated data for $HgCl_2(C_6H_6)_2$ (crystals not yet isolated) has Hg–C distances of 2.813 Å.[13b] Usually, the intermolecular distances are larger in gas-phase structures as the geometry optimizations do not take into account the packing mechanism. Further, the TMB molecules in the calculated structures are tilted toward the mercury atom (TMB/HgR_2 interplanar angles 15–18°), cf. the parallel arrangement observed (interplanar angle 3–4° see above). *Thus, the compression of the mercury–arene contacts to well below the sum of the van der Waals radii is likely to be heavily influenced by the supramolecular interactions present in the crystal packing* (see Supporting Information for a discussion of calculated interaction energies).

Conclusions

Methyl-substituted arenes such as PhMe, TMB or PMB readily form 1:1 $[HgR_2(arene)]$ complexes with a variety of bis(polyfluorophenyl)mercurials. In one case, a unique 1:2 $[HgR_2(arene)_2]$ complex was observed, and other examples of this class could also be prepared by using the methoxy-substituted arene, TMO. In all complexes, structural characterisation showed the presence of Hg···C(arene) or Hg···O(TMO) distances which were just within the van der Waals limits, suggesting only very weak mercury–arene interactions. Furthermore, variation of the *ortho* substituent on the polyfluoroaryl rings of the mercurials (e.g. NO_2, F, H), had little influence upon the respective Hg···C distances. This occurs despite the higher coordination number in the $o\text{-}NO_2$ systems in which there is a strong interaction of one oxygen atom of each nitro group to the mercury atom. It therefore appears that enhanced acceptor properties, owing to the electron-withdrawing effect of the $o\text{-}NO_2$ group, cancels out expected bond lengthening owing to the increase in coordination number. In contrast, the $m\text{-}NO_2$/TMB complex had no Hg–O coordination, but noticeably had the shortest Hg···C(arene) distance along with a different binding mode. The similarity of the $o\text{-}NO_2$/TMB and C_6F_5/TMB systems and the difference of these from the $m\text{-}NO_2$/TMB analogue clearly indicated that steric factors are structurally not determining and this effect is more likely attributable to supramolecular considerations (see below). In addition, the inductive electron-withdrawing effect of the $m\text{-}NO_2$ substituent may contribute to the short Hg···C interaction observed. Within the crystal lattices, the individual $[HgR_2(arene)]$ moieties form canted infinite stacks, with approximately parallel fluoroarene and arene rings, of the form ···HgR_2:arene:HgR_2:arene···, and the

packing of neighbouring stacks exhibit supramolecular associations including fluoroarene–fluoroarene overlap and possible weak C–H···X contacts. Apart from subtle differences, the packing of the [HgR_2(arene)] molecules was largely independent of the R or arene moieties. {The reported[4c] unit-cell parameters for [$Hg(C_6F_5)_2$(naphthalene)] indicate that it is isotypic with [$Hg(C_6F_5)_2$(PhMe)].} The exception was for the C_6F_4-*m*-NO_2 derivatives in which weak C–H···O interactions affected the packing motif. With the higher relative arene content in [HgR_2(arene)$_2$] species, these associate into stacks of the form ···HgR_2:2(arene):HgR_2:2(arene)···, and these do not show the interstack interactions of the 1:1 complexes. However, within each stack there is significant overlap of the near parallel fluoroarene and arene rings which are sufficiently close to be considered as a supramolecular association. Thus, there is evidence that supramolecular interactions are an important feature of these (arene)mercury complexes. In contrast, $HgPh_2$ did not interact with either C_6F_4-*p*-H_2 or $C_6F_5C_6F_5$ under comparable conditions. These systems have the potential for fluoroarene–arene interactions, but, the weaker Lewis acidity of $HgPh_2$ (although adducts with bidentate N-donor ligands have been isolated[21]) and the poorer donor capacity of the polyfluoroarene is expected to inhibit Hg···C interactions.

Experimental Section

General: All solvents were reagent grade and were used as received. The arenes, TMB, PMB, and TMO were obtained from Aldrich and used without further purification. The diorganomercurials, $Hg(C_6F_4$-*o*-$NO_2)_2$, $Hg(C_6F_4$-*m*-$NO_2)_2$, $Hg(C_6F_5)_2$ and $Hg(C_6F_4$-*o*-$H)_2$ were prepared according to literature methods.[3,15] Melting points were determined with an Electrothermal Melting Point apparatus. IR spectra were obtained as Nujol mulls between NaCl plates with a Perkin–Elmer 1600 FTIR instrument. TGA experiments were performed with a Perkin–Elmer Pyris 1 analyser, samples being heated from 30 to 300 °C at 5 °C/min under nitrogen. Solid-sate ^{13}C CPMAS NMR spectra were obtained with a Bruker AM300 spectrometer fitted with a Bruker 4 mm solid-state probe operating at 75.5 MHz; a contact time of 1000 μs with a 3 ms pulse and recycle delay of 1 s was used; MAS spinning speed of 8 kHz eliminated spinning side bands. Chemical shifts were referenced to an external glycine sample. Microanalyses were performed by the Campbell Microanalytical Laboratory, Otago, New Zealand.

[$Hg(C_6F_4$-*o*-$NO_2)_2$(TMB)]: A solution of TMB (0.05 g, 0.4 mmol) in hexane (5 mL) was added to a solution of $Hg(C_6F_4$-*o*-$NO_2)_2$ (0.11 g, 0.20 mmol) in CH_2Cl_2 (10 mL). The mixture was filtered and allowed to concentrate slowly to 1–2 mL yielding pale yellow crystals which were collected by filtration, washed with cold hexane (3 × 1 mL) and dried in air. Yield: 0.10 g (69%). M.p. 178–181 °C. IR (Nujol): $\tilde{\nu}$ = 1611 (w), 1541 (s), 1499 (s), 1455 (vs), 1336 (s), 1317 (m), 1290 (m), 1114 (m), 1048 (s), 1024 (w), 920 (w), 878 (m), 816 (m), 779 (m), 762 (m) cm^{-1}. $C_{22}H_{14}F_8HgN_2O_4$ (722.94): calcd. C 36.55, H 1.95, N 3.88; found C 36.34, H 1.90, N 3.95.

[$Hg(C_6F_4$-*m*-$NO_2)_2$.(TMB)]: A solution of TMB (0.08 g, 0.6 mmol) in hexane (5 mL) was added to a solution of $Hg(C_6F_4$-*m*-$NO_2)_2$ (0.22 g, 0.40 mmol) in CH_2Cl_2 (10 mL). The mixture was filtered and allowed to concentrate slowly to 2–3 mL yielding pale yellow crystals which were collected by filtration, washed with cold hexane (2 mL) and dried in air. Yield: 0.21 g (73%). M.p. 195–198 °C. IR (Nujol): $\tilde{\nu}$ = 1630 (w), 1610 (w), 1553 (s), 1486 (s), 1363 (vs), 1348 (s), 1248 (m), 1082 (s), 1027 (w), 941 (s), 890 (m), 838 (m), 782 (m), 748 (m), 704 (m), 684 (m) cm^{-1}. ^{13}C CPMAS NMR: δ = 137.8 (CMe), 134.9 (CH), 20.0 (Me) ppm; signals for the carbon atoms from the C_6F_4-*m*-NO_2 group were very weak and are not reported. $C_{22}H_{14}F_8HgN_2O_4$ (722.94): calcd. C 36.55, H 1.95, N 3.88; found C 36.59, H 1.96, N 3.80.

[$Hg(C_6F_5)_2$.(TMB)]: A solution of TMB (0.08 g, 0.6 mmol) in hexane (5 mL) was added to a solution of $Hg(C_6F_5)_2$ (0.21 g, 0.40 mmol) in CH_2Cl_2 (10 mL). The mixture was filtered and allowed to concentrate slowly to 2–3 mL yielding colourless crystals which were collected by filtration, washed with hexane (2 mL) and dried in air. Yield: 0.19 g (71%). M.p. 169–172 °C. IR (Nujol): $\tilde{\nu}$ = 1636 (m), 1508 (s), 1272 (m), 1134 (w), 1076 (s), 1066 (s), 1028 (w), 1008 (w), 966 (vs), 882 (m), 806 (m) cm^{-1}. ^{13}C CPMAS NMR: δ = 136.7 (CMe), 134.0 (CH), 20.0 (Me) ppm. Signals for the carbon atoms from the C_6F_5 group were very weak and are not reported. $C_{22}H_{14}F_{10}Hg$ (668.93): calcd. C 39.50, H 2.11; found C 39.54, H 2.24.

[$Hg(C_6F_4$-*o*-H)$_2$.(TMB)]: A solution of TMB (0.08 g, 0.6 mmol) in hexane (5 mL) was added to a solution of $Hg(C_6F_4$-*o*-$H)_2$ (0.20 g, 0.40 mmol) in CH_2Cl_2 (10 mL). The mixture was filtered and allowed to concentrated slowly to 1–2 mL yielding colourless crystals which were collected by filtration, washed with cold hexane (2 × 1 mL) and dried in air. Yield: 0.18 g (70%). M.p. 136–138 °C. IR (Nujol): $\tilde{\nu}$ = 1621 (m), 1594 (w), 1513 (vs), 1343 (w), 1312 (vs), 1348 (s), 1282 (w), 1247 (w), 1205 (m), 1081 (vs), 994 (vs), 983 (s), 896 (w), 880 (m), 864 (m), 808 (m), 702 (m) cm^{-1}. $C_{22}H_{16}F_8Hg$ (632.95): calcd. C 41.75, H 2.55; found C 41.74, H 2.53.

[$Hg(C_6F_4$-*m*-$NO_2)_2$(PMB)]: A solution of PMB (0.09 g, 0.6 mmol) in CH_2Cl_2 (5 mL) was added to a solution of $Hg(C_6F_4$-*m*-$NO_2)_2$ (0.22 g, 0.40 mmol) of CH_2Cl_2 (10 mL). The mixture was filtered and allowed to concentrate slowly to dryness yielding pale yellow crystals which were washed with cold hexane (2 × 2 mL) and dried in air. Yield: 0.15 g (50%). M.p. 139–141 °C. IR (Nujol): $\tilde{\nu}$ = 1630 (m), 1608 (m), 1550 (s), 1486 (s), 1363 (s), 1349 (s), 1249 (m), 1084 (s), 940 (s), 886 (m), 838 (m), 781 (m), 748 (m), 703 (m), 685 (m) cm^{-1}. $C_{23}H_{16}F_8HgN_2O_4$ (736.97): calcd. C 37.48, H 2.19, N 3.80; found C 37.44, H 2.26, N 3.77.

[$Hg(C_6F_5)_2$(PhMe)]. (a): The title complex was initially obtained by concentration of a filtered reaction mixture from a failed redox transmetallation/ligand exchange (containing $Hg(C_6F_5)_2$, ytterbium metal and 3,5-*i*Pr_2pzH[22]) in toluene which gave colourless crystals characterised by X-ray crystallography. The remaining product was not analysed further. **(b):** A solution of $Hg(C_6F_5)_2$ (0.21 g, 0.40 mmol) in PhMe (5 mL) was allowed to concentrate slowly to 0.5 mL yielding colourless crystals identified as the title complex by X-ray crystallography. The crystals rapidly degraded once removed from the mother liquor. The remaining product, the majority of which had crystallised as two large blocks, was removed from the toluene solution and dried briefly in air. Yield 0.14 g (58%). IR (Nujol): $\tilde{\nu}$ = 1637 (m), 1508 (s), 1278 (m), 1070 (s), 1066 (s), 1019 (w), 964 (vs), 807 (m), 728 (m), 694 (w) cm^{-1}. $C_{19}H_8F_{10}Hg$ (626.84): calcd. C 36.41, H 1.29; found C 27.31, H 0.15 [calcd. for $C_{12}F_{10}Hg$ (534.7): C 26.96, H 0.00].

[$Hg(C_6F_4$-*o*-$NO_2)_2$(PhMe)$_2$]: A solution of $Hg(C_6F_4$-*o*-$NO_2)_2$ in PhMe was heated to reflux, then cooled to room temperature and allowed to concentrate slowly. Colourless crystals were obtained which were analysed by X-ray crystallography. Once removed from

the mother liquor, the crystals rapidly degraded and were not analysed further.

[Hg(C$_6$F$_4$-*o*-NO$_2$)$_2$(TMO)$_2$]: A solution of TMO (0.08 g, 0.5 mmol) in of hexane (2 mL) was added to a solution of Hg(C$_6$F$_4$-*o*-NO$_2$)$_2$ (0.11 g, 0.20 mmol) in of CH_2Cl_2 (5 mL). The mixture was filtered and allowed to concentrate slowly to ca. 0.5 mL yielding yellow-orange crystals which were collected by filtration, washed with cold hexane (3 × 1 mL) and dried in air. Yield: 0.14 g (75%). M.p. 122–124 °C. IR (Nujol): $\tilde{\nu}$ = 1611 (w), 1597 (w), 1542 (s), 1509 (s), 1494 (s), 1455 (vs), 1330 (m), 1281 (m), 1228 (m), 1208 (m), 1182 (w), 1158 (m), 1137 (m), 1108 (w), 1049 (m), 1020 (m), 920 (w), 838 (m), 816 (w), 800 (m), 773 (m), 762 (m) cm^{-1}. $C_{30}H_{24}F_8HgN_2O_{10}$ (926.10): calcd. C 38.87, H 2.61, N 3.02; found C 39.41, H 2.71, N 3.00.

[Hg(C$_6$F$_5$)$_2$(TMO)$_2$]: A solution of TMO (0.16 g, 1.0 mmol) in hexane (2 mL) was added to a solution of Hg(C$_6$F$_5$)$_2$ (0.21 g, 0.40 mmol) in of CH_2Cl_2 (5 mL). The mixture was filtered and allowed to concentrate slowly to ca. 0.5 mL yielding colourless crystals which were collected by filtration, washed with cold hexane (3 × 1 mL) and dried in air. Yield: 0.26 g (74%). M.p. 118–120 °C. IR (Nujol): $\tilde{\nu}$ = 1610 (w), 1599 (w), 1511 (s), 1367 (s), 1281 (m), 1260 (w), 1231 (m), 1208 (m), 1183 (w), 1158 (m), 1138 (m), 1064 (m), 1050 (m), 1023 (m), 961 (s), 918 (w), 841 (m), 805 (w), 791 (m), 763 (w), 709 (w) cm^{-1}. ^{13}C CPMAS NMR: δ = 156.4 [C(OMe)], 150.4 [C(OMe)], 144.6 [C(OMe)], 111.2 (CH), 101.6 (CH), 56.8 (OMe) ppm. Signals for the carbon atoms from the C$_6$F$_5$ group were very weak and are not reported. $C_{30}H_{24}F_{10}HgO_6$ (871.08): calcd. C 41.37, H 2.78; found C 41.52, H 2.97.

Theoretical Procedures: The optimizations were performed at B3LYP/6-31+G(d) the level by using the GAUSSIAN 03 package.[23] In order to describe the core electrons of Hg we employed the Stuttgart/Dresden effective core potential (ECP) with a Dirac-Fock relativistic correction, abbreviated MDF, as implemented in GAUSSIAN 03. The number of electrons included in the core was 60. For the valence electrons on Hg we used a double-ζ basis set optimized for the chosen ECP.

X-ray Structure Determinations: Single crystals suitable for X-ray analysis were covered in viscous oil and mounted on a glass fibre. Data ($2\theta_{max}$ = 55°) were collected at 123(1) K by using a Nonius KAPPA or Bruker X8 Apex CCD system and Mo-K_α (λ 0.71073 Å) radiation. After integration and scaling, data sets were merged (R_{int} as quoted) and the structures were solved by using conventional methods and refined by full-matrix least squares using the SHELX-97 software,[24a] in conjunction with the X-Seed interface.[24b] Non-hydrogen atoms were refined with anisotropic thermal parameters, and hydrogen atoms were placed in calculated positions. Data were corrected for absorption by using SORTAV[24c] or SADABS.[24d] CCDC-691185, -691186, -691187, -691188, -691189, -691190, -691191, -691192, -691193 contain the supplementary crystallographic data for this paper. These data can be obtained free of charge from The Cambridge Crystallographic Data Centre via www.CCDC.cam.ac.uk/data_request/cif.

Crystal and Refinement Data

[Hg(C$_6$F$_4$-*o*-NO$_2$)$_2$(TMB)]: $C_{22}H_{14}F_8HgN_2O_4$ (722.94). Monoclinic, $P2_1/n$. a = 10.1573(4), b = 6.9776(3), c = 15.8011(7) Å, β = 103.525(1)°. V = 1088.82(8) Å^3. Z = 2. $D_{calcd.}$ = 2.205 g cm^{-3}. μ = 7.17 mm^{-1}, N_t = 7587, N = 2493 (R_{int} = 0.022). R_1 = 0.016 ($I > 2\sigma I$), wR_2 = 0.038 (all data).

[Hg(C$_6$F$_4$-*m*-NO$_2$)$_2$(TMB)]: $C_{22}H_{14}F_8HgN_2O_4$ (722.94). Monoclinic, $P2_1/n$. a = 10.6875(2), b = 6.8261(2), c = 15.8748(3) Å, β = 106.504(1)°. V = 1110.41(4) Å^3. Z = 2. $D_{calcd.}$ = 2.162 g cm^{-3}. μ = 7.03 mm^{-1}, N_t = 12584, N = 2526 (R_{int} = 0.030). R_1 = 0.024 ($I > 2\sigma I$), wR_2 = 0.048 (all data).

[Hg(C$_6$F$_5$)$_2$(TMB)]: $C_{22}H_{14}F_{10}Hg$ (668.92). Monoclinic, $P2_1/n$. a = 6.9203(1), b = 10.0756(2), c = 14.8125(3) Å, β = 100.105(2)°. V = 1016.80(3) Å^3. Z = 2. $D_{calcd.}$ = 2.185 g cm^{-3}. μ = 7.67 mm^{-1}, N_t = 10835, N = 2272 (R_{int} = 0.060). R_1 = 0.034 ($I > 2\sigma I$), wR_2 = 0.099 (all data).

[Hg(C$_6$F$_4$-*o*-H)$_2$(TMB)]: $C_{22}H_{16}F_8Hg$ (632.94). Monoclinic, $P2_1/n$. a = 6.9802(1), b = 10.1317(2), c = 14.4297(3) Å, β = 101.011(1)°. V = 1001.70(3) Å^3. Z = 2. $D_{calcd.}$ = 2.098 g cm^{-3}. μ = 7.76 mm^{-1}, N_t = 9927, N = 2295 (R_{int} = 0.046). R_1 = 0.023 (I>2σI), wR_2 = 0.059 (all data).

[Hg(C$_6$F$_4$-*m*-NO$_2$)$_2$(PMB)]: $C_{23}H_{16}F_8HgN_2O_4$ (736.97). Monoclinic, $P2_1/n$. a = 10.5936(5), b = 7.1147(4), c = 16.2384(3) Å, β = 108.246(2)°. V = 1162.4(1) Å^3. Z = 2. $D_{calcd.}$ = 2.106 g cm^{-3}. μ = 6.72 mm^{-1}, N_t = 11792, N = 2661 (R_{int} = 0.036). R_1 = 0.028 ($I > 2\sigma I$), wR_2 = 0.073 (all data). Note: the PMB molecule was modeled as disordered over the inversion centre with the substituent at C(7) being 50% CH_3 and 50% H; similarly, the NO_2 group was modeled as disordered over two positions (with occupancy fixed at 0.50 and restrained geometry), rotated by approximately 90° along the N–C bond; thermal ellipsoids for C(4), C(5), F(2), and F(3) were elongated approximately perpendicular to the ring plane which suggested that the entire C$_6$F$_4$-*m*-NO_2 moiety was disordered, but this could not be adequately modeled; attempted refinements in lower symmetry space groups were less satisfactory than the current solution.

[Hg(C$_6$F$_5$)$_2$(PhMe)]: $C_{19}H_8F_{10}Hg$ (626.84). Monoclinic, $P2_1/c$. a = 9.5319(7), b = 6.8463(5), c = 14.5789(12) Å, β = 104.831(2)°. V = 919.70(12) Å^3. Z = 2. $D_{calcd.}$ = 2.264 g cm^{-3}. μ = 8.47 mm^{-1}, N_t = 10626, N = 2112 (R_{int} = 0.024). R_1 = 0.019 ($I > 2\sigma I$), wR_2 = 0.042 (all data).

[Hg(C$_6$F$_4$-*o*-NO$_2$)$_2$(PhMe)$_2$]: $C_{26}H_{16}F_8HgN_2O_4$ (773.00). Triclinic, $P(-1)$. a = 7.5864(1), b = 8.2200(2), c = 11.5733(3) Å, α = 84.279(1), β = 74.206(1), γ = 64.319(1)°. V = 625.73(2) Å^3. Z = 1. $D_{calcd.}$ = 2.051 g cm^{-3}. μ = 6.25 mm^{-1}, N_t = 9472, N = 2795 (R_{int} = 0.038). R_1 = 0.043, ($I > 2\sigma I$), wR_2 = 0.105 (all data).

[Hg(C$_6$F$_4$-*o*-NO$_2$)$_2$(TMO)$_2$]: $C_{30}H_{24}F_8HgN_2O_{10}$ (926.10. Monoclinic, $P2_1/c$. a = 7.1329(4), b = 15.3765(8), c = 14.0442(7) Å, β = 92.415(1)°. V = 1538.99(14) Å^3. Z = 2. $D_{calcd.}$ = 1.996 g cm^{-3}. μ = 5.112 mm^{-1}, N_t = 17253, N = 3532 (R_{int} = 0.031). R_1 = 0.031, ($I > 2\sigma I$), wR_2 = 0.057 (all data).

[Hg(C$_6$F$_5$)$_2$(TMO)$_2$]: $C_{30}H_{24}F_{10}HgO_6$ (871.08. Monoclinic, $P2_1/c$. a = 6.9447(2), b = 15.7351(4), c = 13.5720(4) Å, β = 96.475(1)°. V = 1473.63(7) Å^3. Z = 2. $D_{calcd.}$ = 1.963 g cm^{-3}. μ = 5.330 mm^{-1}, N_t = 11834, N = 3358 (R_{int} = 0.022). R_1 = 0.026, ($I > 2\sigma I$), wR_2 = 0.050 (all data).

Supporting Information (see also the footnote on the first page of this article): Ellipsoid plots and structural details for [Hg(C$_6$F$_5$)$_2$-(TMB)], [Hg(C$_6$F$_4$-*o*-H)$_2$(TMB)], [Hg(C$_6$F$_4$-*m*-NO$_2$)$_2$(PMB)] and [Hg(C$_6$F$_5$)$_2$(TMO)$_2$] and a discussion of the calculated interaction energies for (arene)mercury complexes.

Acknowledgments

We thank the Australian Research Council for financial support and Dr. Jenny Pringle for assistance with solid state NMR measurements. E. I. gratefully acknowledges general allocations of

computing time from the Facility of the Australian Partnership for Advanced Computing. J. H. and K. R. S. gratefully acknowledge funding from the National Science Foundation (CHE0505863).

[1] a) S. C. Cohen, A. G. Massey, *Adv. Fluorine Chem.* **1970**, *6*, 83–285; b) E. Y.-X. Chen, T. J. Marks, *Chem. Rev.* **2000**, *100*, 1391–1434; c) A. Y. Timoshkin, G. Frenking, *Organometallics* **2008**, *27*, 371–380, and references therein.

[2] a) A. Guerrero, E. Martin, D. L. Hughes, N. Kaltsoyannis, M. Bochmann, *Organometallics* **2006**, *25*, 3311–3313; b) A. Sundararamen, R. A. Lalancette, L. N. Zakharov, A. L. Rheingold, F. Jäkle, *Organometallics* **2003**, *22*, 3526–3532; c) G. S. Hair, A. H. Cowley, R. A. Jones, B. G. McBurnett, A. Voigt, *J. Am. Chem. Soc.* **1999**, *121*, 4922–4923.

[3] G. B. Deacon, J. E. Cosgriff, E. T. Lawrenz, C. M. Forsyth, D. L. Wilkinson in *Synthetic Methods of Organometallic and Inorganic Chemistry (Herrmann/Brauer)* (Ed.: W. A. Herrman), Thieme, New York, **1997**, vol. 6 (vol. Ed.: F. T. Edelmann), p. 48–51.

[4] a) F. Schulz, I. Pantenburg, D. Naumann, *Z. Anorg. Allg. Chem.* **2003**, *629*, 2312–2316; b) F. Schulz, D. Naumann, *Z. Anorg. Allg. Chem.* **2005**, *631*, 715–718; c) C. N. Burress, M. I. Bodine, Q. Elbjeirami, J. H. Reibenspies, M. A. Omary, F. P. Gabbaï, *Inorg. Chem.* **2007**, *46*, 1388–1395.

[5] a) M. Tsunoda, F. P. Gabbaï, *J. Am. Chem. Soc.* **2000**, *122*, 8335–8336; b) M. R. Haneline, M. Tsunoda, F. P. Gabbaï, *J. Am. Chem. Soc.* **2002**, *124*, 3737–3742; c) M. R. Haneline, J. B. King, F. P. Gabbaï, *Dalton Trans.* **2003**, 2686–2690; d) M. A. Omary, R. M. Kassab, M. R. Haneline, O. Elbjeirami, F. P. Gabbaï, *Inorg. Chem.* **2003**, *42*, 2176–2178; e) T. J. Thomas, V. I. Bakhmutov, F. P. Gabbaï, *Angew. Chem. Int. Ed.* **2006**, *45*, 7030–7033; f) I. A. Tikhonova, K. I. Tugashov, F. M. Dolgushin, A. A. Yakovenko, B. N. Strunin, P. V. Petrovskii, G. G. Furin, V. B. Shur, *Inorg. Chim. Acta* **2006**, *359*, 2728–2735; g) T. J. Thomas, C. N. Burress, L. Pandey, F. P. Gabbaï, *Dalton Trans.* **2006**, 4654–4656; h) T. J. Taylor, C. N. Burress, F. P. Gabbaï, *Organometallics* **2007**, *26*, 5252–5263.

[6] a) J. W. Steed, D. R. Turner, K. J. Wallace, *Core Concepts in Supramolecular and Nanochemistry*, Wiley, Chichester, **2007**; b) L. F. Lindoy, I. M. Atkinson, *Self Assembly in Supramolecular Systems*, Cambridge University Press, UK, **2000**.

[7] a) S. Lorenzo, G. R. Lewis, I. Dance, *New J. Chem.* **2000**, *24*, 295–304; b) Y. Sun, W. E. Piers, M. Parvez, *Can. J. Chem.* **1998**, *76*, 513–517; c) A. J. Mountford, S. J. Lancaster, S. J. Coles, P. N. Horton, D. L. Hughes, M. B. Hursthouse, M. E. Light, *Organometallics* **2006**, *25*, 3837–3847; d) J. M. Blackwell, W. E. Piers, M. Parvez, R. McDonald, *Organometallics* **2002**, *21*, 1400–1407; e) A. J. Mountford, S. J. Lancaster, S. J. Coles, P. N. Horton, D. L. Hughes, M. B. Hursthouse, M. E. Light, *Inorg. Chem.* **2005**, *44*, 5921–5933.

[8] From the atomic coordinates deposited in the CSD,[9a] analyses of the packing of reported (polyfluorophenyl)mercury compounds showed significant alignment of the fluoroarene–fluoroarene or fluoroarene–arene ring planes in many instances, indicating possible supramolecular interactions as a structural component in the planar and twisted examples of HgR_2 compounds.[9]

[9] a) *The Cambridge Structural Database*, **2006**, version 5.27; b) D. S. Brown, A. G. Massey, D. A. Wickens, *J. Organomet. Chem.* **1980**, *194*, 131–135; c) N. R. Kuchner, M. Mathew, *J. Chem. Soc., Chem. Commun.* **1966**, 71–73; d) D. L. Wilkinson, J. Riede, G. Müller, *Z. Naturforsch., Teil B* **1991**, *46*, 285–288; e) G. B. Deacon, C. M. Forsyth, D. M. M. Freckmann, G. Meyer, D. Stellfeldt, *Z. Anorg. Allg. Chem.* **2000**, *626*, 540–546; f) D. Naumann, F. Schulz, *Z. Anorg. Allg. Chem.* **2005**, *631*, 122–125; g) G. B. Deacon, P. W. Felder, P. C. Junk, K. Müller-Buschbaum, T. J. Ness, C. Quitmann, *Inorg. Chim. Acta* **2005**, *358*, 4389–4393; h) G. B. Deacon, P. C. Junk, *J. Chem. Crystallogr.* **2003**, *33*, 605–607.

[10] a) C. R. Patrick, G. S. Prosser, *Nature* **1960**, *187*, 1021; b) J. H. Williams, *Acc. Chem. Res.* **1993**, *26*, 593–598, and references therein.

[11] a) D. Grdenić, *Q. Rev., Chem. Soc.* **1965**, *19*, 303–328; b) A. Bondi, *J. Phys. Chem.* **1964**, *68*, 441–451; c) A. J. Canty, G. B. Deacon, *Inorg. Chim. Acta* **1980**, *45*, L225–L227; d) S. S. Batsanov, *J. Chem. Soc., Dalton Trans.* **1998**, 1541–1546; e) L. Pauling in *The Nature of the Chemical Bond*, 3rd ed., Cornell University Press, Ithaca, New York, **1960**; f) S. C. Nyburg, C. H. Faerman, *Acta Crystallogr., Sect. B* **1985**, *41*, 274–279.

[12] a) M. Niemeyer, P. P. Power, *Organometallics* **1997**, *16*, 3258–3260; b) M. Hoerner, A. J. Bortoluzzi, J. Beck, M. Serafin, *Z. Anorg. Allg. Chem.* **2002**, *628*, 1104–1107; c) M. Hoerner, G. M. Oliveira, L. C. Visentin, R. S. Cezar, *Inorg. Chim. Acta* **2006**, *359*, 4667–4671; d) M. Hoerner, G. M. Oliveira, E. G. Koehler, G. Eduardo, L. C. Visentin, *J. Organomet. Chem.* **2006**, *691*, 1311–1314; e) M. Hoerner, F. Boch, L. C. Visentin, *Z. Anorg. Allg. Chem.* **2007**, *633*, 1779–1782.

[13] a) W. Lau, J. C. Huffman, J. K. Kochi, *J. Am. Chem. Soc.* **1982**, *104*, 5515–5517; b) A. S. Borovik, S. G. Bott, A. R. Barron, *Angew. Chem. Int. Ed.* **2000**, *39*, 4117–4118; c) A. S. Borovik, S. G. Bott, A. R. Barron, *J. Am. Chem. Soc.* **2001**, *123*, 11219–11228; d) L. C. Damude, P. A. W. Dean, *J. Chem. Soc., Chem. Commun.* **1978**, 1083–1084; e) L. C. Damude, P. A. W. Dean, *J. Organomet. Chem.* **1979**, *181*, 1–15; f) L. C. Damude, P. A. W. Dean, M. D. Sefcik, J. Scheafer, *J. Organomet. Chem.* **1982**, *226*, 105–114.

[14] a) W. R. Scheidt, M. E. Kastner, K. Hatano, *Inorg. Chem.* **1978**, *17*, 706–710; b) W. R. Scheidt, C. A. Reed, *Inorg. Chem.* **1978**, *17*, 710–714.

[15] a) H. B. Albrecht, G. B. Deacon, *J. Organomet. Chem.* **1973**, *57*, 77–86; b) G. B. Deacon, D. Tunaley, *J. Organomet. Chem.* **1978**, *156*, 403–426; c) J. Baldumus, G. B. Deacon, C. M. Forsyth, E. Izgorodina, P. C. Junk, G. Meyer, I. Pantenburg, unpublished results.

[16] M. A. Bennett, M. Contel, D. C. R. Hockless, L. L. Welling, A. C. Willis, *Inorg. Chem.* **2002**, *41*, 844–855.

[17] M. Tschinkl, A. Schier, J. Riede, F. P. Gabbaï, *Organometallics* **1999**, *18*, 2040–2042.

[18] J. D. Dunitz, R. Taylor, *Chem. Eur. J.* **1997**, *3*, 89–98.

[19] a) G. Althoff, J. Ruiz, V. Rodriguez, G. López, J. Pérez, C. Janiak, *Cryst. Eng. Commun.* **2006**, *8*, 662–665; b) M. C. W. Chan, S. C. F. Kui, J. M. Cole, G. J. McIntyre, S. Matsui, N. Zhu, K.-H. Tam, *Chem. Eur. J.* **2006**, *12*, 2607–2619.

[20] a) I. A. Tikhonova, K. I. Tugashov, F. M. Dolgushin, A. A. Yakovenko, P. V. Petrovskii, G. G. Furin, A. P. Zaraisky, V. B. Shur, *J. Organomet. Chem.* **2006**, *692*, 953–962; b) I. A. Tikhonova, F. M. Dolgushin, K. I. Tugashov, P. V. Petrovskii, G. G. Furin, V. B. Shur, *J. Organomet. Chem.* **2002**, *654*, 123–131; c) J. Baldamus, G. B. Deacon, E. Hey-Hawkins, P. C. Junk, C. Martin, *Aust. J. Chem.* **2002**, *55*, 195–198; d) J. B. King, M. Tsunoda, F. P. Gabbaï, *Organometallics* **2002**, *21*, 4201–4205; e) J. B. King, M. R. Haneline, M. Tsunoda, F. P. Gabbaï, *J. Am. Chem. Soc.* **2002**, *124*, 9350–9351; f) M. R. Haneline, F. P. Gabbaï, *Inorg. Chem.* **2005**, *44*, 6248–6255; g) I. A. Tikhonova, F. M. Dolgushin, A. A. Yakovenko, K. I. Tugashov, P. V. Petrovskii, G. G. Furin, V. B. Shur, *Organometallics* **2005**, *24*, 3395–3400.

[21] a) G. B. Deacon, A. J. Canty, *Inorg. Nucl. Chem. Lett.* **1969**, *5*, 183–185; b) A. J. Canty, G. B. Deacon, *J. Organomet. Chem.* **1973**, *49*, 125–132; c) A. J. Canty, B. M. Gatehouse, *Acta Crystallogr., Sect. B* **1972**, *28*, 1872–1888.

[22] J. Hitzbleck, G. B. Deacon, K. Ruhlandt-Senge, *Eur. J. Inorg. Chem.* **2007**, 592–601.

[23] M. J. Frisch, G. W. Trucks, H. B. Schlegel, G. E. Scuseria, M. A. Robb, J. R. Cheeseman, J. A. Montgomery Jr, T. Vreven, K. N. Kudin, J. C. Burant, J. M. Millam, S. S. Iyengar, J. Tomasi, V. Barone, B. Mennucci, M. Cossi, G. Scalmani, N. Rega, G. A. Petersson, H. Nakatsuji, M. Hada, M. Ehara, K. Toyota, R. Fukuda, J. Hasegawa, M. Ishida, T. Nakajima, Y. Honda,

O. Kitao, H. Nakai, M. Klene, X. Li, J. E. Knox, H. P. Hratchian, J. B. Cross, V. Bakken, C. Adamo, J. Jaramillo, R. Gomperts, R. E. Stratmann, O. Yazyev, A. J. Austin, R. Cammi, C. Pomelli, J. W. Ochterski, P. Y. Ayala, K. Morokuma, G. A. Voth, P. Salvador, J. J. Dannenberg, V. G. Zakrzewski, S. Dapprich, A. D. Daniels, M. C. Strain, O. Farkas, D. K. Malick, A. D. Rabuck, K. Raghavachari, J. B. Foresman, J. V. Ortiz, Q. Cui, A. G. Baboul, S. Clifford, J. Cioslowski, B. B. Stefanov, A. L. G. Liu, P. Piskorz, I. Komaromi, R. L. Martin, D. J. Fox, T. Keith, M. A. Al-Laham, C. Y. Peng, A. Nanayakkara, M. Challacombe, P. M. W. Gill, B. Johnson, W. Chen, M. W. Wong, C. Gonzalez, J. A. Pople, *GAUSSIAN 03*, Revision C.02, Gaussian, Inc., Wallingford CT, **2004**.

[24] a) G. M. Sheldrick, *SHELX-97: Program for crystal structure solution and refinement*, University of Göttingen, **1997**; b) L. J. Barbour, *J. Supramol. Chem.* **2001**, *1*, 189–191; c) R. H. Blessing, *J. Appl. Crystallogr.* **1997**, *30*, 421–426; d) G. M. Sheldrick, *SADABS: Program for scaling and absorption correction of area detector data*, University of Göttingen, **1997**.

Received: June 17, 2008
Published Online: September 4, 2008

